High bias voltage effect on spin-dependent conductivity and shot noise in carbon-doped Fe(001)/MgO(001)/Fe(001) magnetic tunnel junctions

R. Guerrero, D. Herranz, and F. G. Aliev[a)]
Departamento de Fisica de la Materia Condensado C-III, Universidad Autonoma de Madrid, 28049 Madrid, Spain

F. Greullet, C. Tiusan, M. Hehn, and F. Montaigne
Laboratoire de Physique des Matériaux, UMR CNRS 7556, Nancy Université, Bd. des Aiguillettes, B.P. 239, 54506 Vandœuvre-lès-Nancy Cedex, France

(Received 14 June 2007; accepted 11 September 2007; published online 26 September 2007)

Low temperature (10 K) high voltage bias dynamic conductivity (up to 2.7 V) and shot noise (up to 1 V) were studied in epitaxial Fe(100)/Fe–C/MgO(100)/Fe(100) magnetic tunnel junctions as a function of the magnetic state. The junctions show large tunnel magnetoresistance (185% at 300 K and 330% at 4 K). Multiple sign inversion of the magnetoresistance is observed for bias polarity when the electrons scan the electronic structure of the bottom Fe–C interface. The shot noise shows a Poissonian character. This demonstrates a pure spin-dependent direct tunneling mechanism and validates the high structural quality of the MgO barrier. © *2007 American Institute of Physics*.
[DOI: 10.1063/1.2793619]

Magnetic tunnel junctions[1,2] (MTJs) are nowadays one of the most active areas of material science and spintronics. Recent theoretical predictions[3,4] and experimental demonstrations[5–9] of coherent spin-dependent tunneling in single crystal Fe(100)/MgO(100)/Fe(100) MTJs revolutionized this area. The large tunneling magnetoresistance (TMR) at low bias voltages is mostly due to fully spin polarized Δ_1 bulk electron states in Fe(001), reflected for antiparrallel (AP) ferromagnetic electrodes configuration or well transmitted for the parallel (P) state.[3,4] However, the tunneling mechanism gets more complex when taking into account the electronic structure of the interfaces[10] and when biasing the junction. Therefore, for finite bias polarities, the antiparallel conductance may exceed the parallel one, resulting in TMR suppression[8] or its sign reversal.[10] By engineering the chemical and electronic structure of the Fe/MgO interface, the voltage variation of the TMR in amplitude and sign can be skilfully manipulated. It has been recently demonstrated that the carbon doping of the bottom Fe/MgO interface leads to a strongly asymmetric TMR versus bias, providing a root for the creation of high-output voltage device applications.[9]

Our letter presents a first study of dynamical conductance and TMR in a large bias window, up to 2.7 V, for Fe(100)/Fe–C/MgO(100)/Fe(100) MTJs. The shot noise analysis in different magnetization configurations is performed at voltages up to 1 V. The experiments are done at room temperature (300 K) and low temperature (4–10 K). The measured TMR ratio increases from 185% at 300 K to 330% at 4 K. Our tunneling spectroscopy experiments show a clear maximum in the AP conductivity for a finite bias and a multiple TMR sign inversion. Furthermore, in both P and AP configurations, the shot noise measurements demonstrate an uncorrelated direct tunneling mechanism across the MgO barrier. The shot noise analysis and the large breakdown voltage of the junctions (up to 3 V) demonstrates the high quality of our MgO barriers (i.e., absence of defects such as oxygen vacancies).

Our epitaxial Fe(45 nm)/MgO(3 nm)/Fe(10 nm)/Co(20 nm)/Pd(10 nm)/Au(10 nm) samples were grown by molecular beam epitaxy on MgO(100) substrates under UHV condition (4×10^{-11} mbar base pressure). Prior to deposition, the substrate is annealed at 600°; then the layers are grown at room temperature. For flattening, the Fe electrodes are annealed to 450° (bottom Fe) and 380° (top Fe). Following the growth procedure of Ref. 13, two different samples can be grown: samples with clean Fe/MgO bottom interfaces and samples with carbon doping at bottom Fe/MgO interface (Fe/Fe–C/MgO). The Reflection high-energy electron diffraction (RHEED) analysis performed on each layer of the MTJ stack allows a direct control of the epitaxial growth and the high crystalline quality of the epitaxial layers. Compared to clean samples, in the samples with carbon, the bottom Fe(001) electrode presents a $c(2\times2)$ surface reconstruction (Fig. 1). The RHEED, however, showed no clear evidence of any structural difference between the two systems. This opens perspectives for further analysis which should involve techniques with local "resolution:" x-ray appearance near-edge structum extended x-ray absaptie fine structure surface x-Ray diffraction, etc. After the growth of the multilayer stack, MTJs with micrometric lateral size have been patterned using standard optical lithography/ion etching process. All the MTJs studied here contain carbon doped Fe/MgO interface. They have shown a large voltage stability of up to 3 V. The larger stability of the junctions with carbon

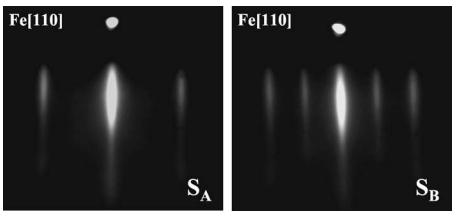

FIG. 1. RHEED patterns of the Fe bottom layer for (a) carbon-free Fe and (b) Fe/Fe–C along the [110] crystallographic direction. Additional pattern for Fe/Fe–C surface demonstrate the $c(2\times2)$ reconstruction related to carbon.

[a)]Electronic mail: farkhad.aliev@uam.es

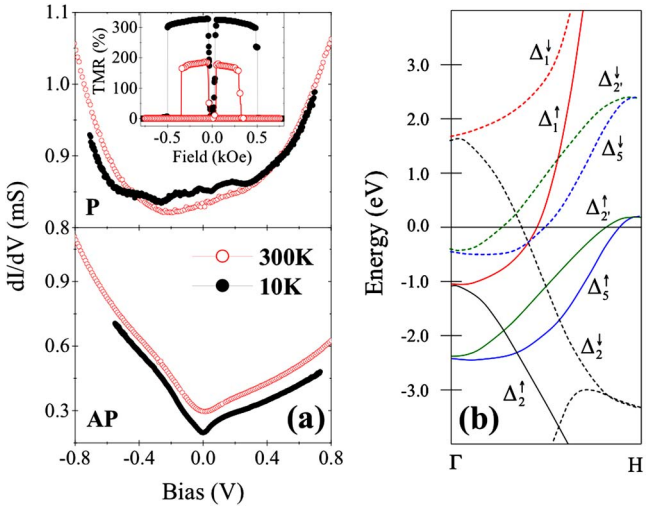

FIG. 2. (Color online) (a) Dynamic conductivities in P (top panel) and AP (bottom panel) magnetization states at 300 K (open circles) and 10 K (full circles). Top panel inset: TMR curves at 300 K (red open circles) and 4 K (black full circles). (b) Bulk band structure diagram of bcc Fe.

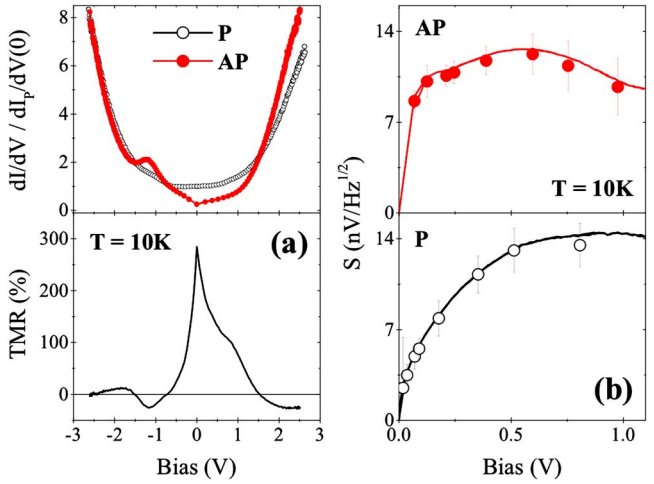

FIG. 3. (Color online) (a) Dynamic conductivities at 10 K (top panel) and related TMR (V) (bottom panel). (b) Shot noise measurements in P and AP states measured at 10 K in bias when the electrons are injected from the top toward the bottom MTJ electrode [negative voltage in Figs. 2 and 3(a)].

at the Fe/MgO interface has been observed performing experiments on more than ten junctions belonging to different sets of wafers.

Dynamic conductance $G(V)$ and shot noise bias dependence have been studied using a four-probe method with a setup allowing us to vary the temperature between 2 and 300 K, equipped with preamplifiers situated on top of the cryostat. Two different techniques were employed to measure dynamic conductance in P or AP states, providing nearly identical results. In the first, the MTJ is biased by dc voltage with superimposed low amplitude sinusoidal wave ($V_{ac}<20$ mV). The second technique, mainly employed at high bias, uses square current wave superimposed on dc current. Shot noise measurements were done using a cross-correlation technique. More details of setup were published elsewhere.[11,12]

At 300 K, the Fe/Fe–C/MgO(3 nm)/Fe/Co MTJs show RA product values (RT) ranging from 0.42 to 0.48 MΩ μm^2. The inset in the top panel of Fig. 2 shows typical TMR curves measured at 10 mV either at 300 K and at 4 K. The large TMR ratio of 185% at 300 K indicates the high quality of the MTJs. Interestingly, the low temperature TMR (~330%) notably exceeds previously reported (250%) maximum values of zero-bias TMR in epitaxial Fe(100)/MgO/Fe MTJs with "undopped" Fe/MgO interfaces.[8] The temperature variation of the TMR is understood from the dynamic conductivity experiments $G=dI/dV$ shown in Fig. 2(a), which plots $G(V)$ at 300 and 10 K within a voltage range of 0.8 V. Firstly, asymmetric $G(V)$ characteristics in positive and negative voltages demonstrate different electronic structures of the top and bottom electrodes and Fe/MgO interfaces.[9] Secondly, we claserve significantly different temperature variations of conductivity in P and AP magnetization configurations. In the AP configuration [Fig. 2(b)], we claserve almost no temperature dependent shape variation, except the enhancement of low bias anomaly at 10 K. However, we notice a strong reduction of $G_{AP}(V)$ by 50% at low temperature. On the other hand, a net temperature dependent shape variation between 300 and 10 K [Fig. 2(a), top panel] is clearly seen for $G_P(V)$. Interestingly, the zero bias G_P is mostly constant with temperature (only 2% variation). Additional local minima appear at 10 K for both positive and negative finite bias voltages. At low temperature, all studied MTJs reveal novel P-state low-bias conductance oscillations with about four minima [Fig. 2(a), top panel]. We note that low-bias conductivity minima in the P state have been already observed in carbon-free samples even at 300 K. However, we always measured only two local conductance minima.[13] These minima were explained by the Δ_5 majority electron contribution to the total conductivity at low voltage [<0.3 eV, which is the top of the majority Δ_5 band [Fig. 2(b)]. The origin of low temperature $G_P(V)$ minima observed in Fe/Fe–C/MgO/Fe MTJs opens interesting theoretical perspectives.

Figure 3(a) presents high bias conductance for voltages up to 2.7 V, measured at 10 K. The influence of joule heating (few Kelvins) on the I-V's is neglected due to the rather weak observed low temperature dependence of both G_P and G_{AP}. Interestingly, while $G_P(V)$ is rather symmetric, in negative voltage when the electrons tunnel into the bottom Fe–C/MgO electrode, the $G_{AP}(V)$ shows a strong asymmetric local maximum superimposed on roughly parabolic background. This "local" resonant increase of the G_{AP} ($G_{AP}>G_P$) in a narrow[14] energy window will lead to the lower voltage sign reversal of the TMR [Fig. 3(a), bottom panel]. Similar to scanning tunneling spectroscopy experiments,[15] and as we have previously shown,[10] the resonant enhancement of G_{AP} is attributed to the contribution to the tunneling of the Fe minority interfacial resonance (IRS). However, we only observed this phenomena in carbon-free Fe/MgO/Fe samples with thinner MgO barrier, where the Fe IRS still significantly contributes to the tunneling.[16] In the samples studied here, having carbon at the Fe–C/MgO interface, an important effect of the G_{AP} resonant activation by IRS is observed even for 3 nm thick MgO barriers. To elucidate this interesting property, theoretical investigation of two effects is in progress: (i) the effect of Fe–C–MgO bounding on the minority spin Fe(001) IRS (i.e., shift in energy and dispersion in k) and (ii) the carbon induced periodical perturbation of the potential at the bottom Fe/MgO interface (i.e., $c(2\times2)$ reconstruction, Fig. 1) induces scat-

tering events which change k vector. This has direct consequences on the total conductivity.

In positive bias, when electrons are injected toward the top electrode, the low bias TMR changes the sign above 1.5 V. This is determined by the G_{AP} strong enhancement when, in the AP configuration, the injected Δ_1 electrons from the bottom Fe electrode arrive as hot electrons in the top electrode and find an equivalent symmetry in the minority band. In negative voltage, when electrons tunnel into the bottom Fe–C/MgO electrode, similar contribution of the minority Δ_1 symmetry to the conductivity is expected. However, the TMR second sign reversal seems to appear at much higher voltages, above 2.5 V [Fig. 3(a), bottom panel]. One possible reason would be the reduction of the hot electron thermalization length in the bottom electrode. The effect of the IRS at Fe–C/MgO interface on this phenomena requires further theoretical investigation.

Figure 3(b) presents shot noise measurements carried out at $T=10$ K on Fe/Fe–C/MgO/Fe MTJs, with bias direction corresponding to the injection of electrons from the top to the bottom (carbon doped) Fe/MgO interface. For comparison, the solid curves show the "theoretical" expectation for the shot noise, for electron tunneling having Poissonian character: $S_V=2e\langle I\rangle/G^2$, with G as the dynamic conductivity [Fig. 3(a)] and I as the applied current. Within the error bars, showing dispersion of the shot noise "white" spectrum in the kilohertz range, the experimental data clearly indicate the absence of electron correlations and/or sequential tunneling phenomena. This proves that both P and AP spin-dependent conductances and the shot noise are due to direct tunneling between electron bands, as expected for the coherent tunneling.[17] The absence of resonant assisted tunneling in the shot noise demonstrates the high quality of our epitaxial MgO barriers (i.e., the absence of oxygen vacancies). This high quality is furthermore confirmed by the large breakdown voltage of the MTJs (up to 3 V).

The authors thank G. Lengaigne for technological process of MTJs. The work in Madrid has been supported by Spanish-French Integrated Action project (HF2006-0039), Spanish MEC(MAT2006-07196), and Comunidad de Madrid (S-505/MAT0194). This work, as a part of the European Science Foundation EUROCORES Programme 05-FONE-FP-010-SPINTRA, was also supported by funds from the Spanish MEC (MAT2006-28183-E) and the EC Sixth Framework Programme under Contract No. ERAS-CT-2003-980409.

[1] J. S. Moodera, L. R. Kinder, T. M. Wong, and R. Meservey, Phys. Rev. Lett. **74**, 3273 (1995).
[2] T. Miyazaki and N. Tezuka, J. Magn. Magn. Mater. **139**, L231 (1995).
[3] W. H. Butler, X. G. Zang, T. C. Schulthess, and J. M. MacLaren, Phys. Rev. B **63**, 054416 (2001).
[4] J. Mathon and A. Umerski, Phys. Rev. B **63**, 220403R (2001).
[5] M. Bowen, V. Cros, F. Petroff, A. Fert, C. Martínez Boubeta, J. L. Costa-Krämer, J. V. Anguita, A. Cebollada, F. Briones, J. M. de Teresa, L. Morellón, M. R. Ibarra, F. Güell, F. Peiró, and A. Cornet, Appl. Phys. Lett. **79**, 1655 (2001).
[6] J. Faure-Vincent, C. Tiusan, E. Jouguelet, F. Canet, M. Sajieddin, C. Bellouard, E. Popova, M. Hehn, F. Montaigne, and A. Schuhl, Appl. Phys. Lett. **82**, 4507 (2003).
[7] S. S. P. Parkin, C. Kaiser, A. Panchula, P. M. Rice, B. Hughes, M. Samant, and S. H. Yang, Nat. Mater. **3**, 862 (2004).
[8] S. Yuasa, T. Nagahama, A. Fukushima, Y. Suzuki, and K. Ando, Nat. Mater. **3**, 868 (2004).
[9] C. Tiusan, M. Sicot, M. Hehn, C. Bellouard, S. Andrieu, F. Montaigne, and A. Schuhl, Appl. Phys. Lett. **88**, 062512 (2006).
[10] C. Tiusan, J. Faure-Vincent, C. Bellouard, M. Hehn, E. Jouguelet, and A. Schuhl, Phys. Rev. Lett. **93**, 106602 (2004).
[11] R. Guerrero, F. G. Aliev, R. Villar, J. Hauch, M. Fraune, G. Güuntherodt, K. Rott, H. Bückl, and G. Reiss, Appl. Phys. Lett. **87**, 042501 (2005).
[12] R. Guerrero, F. G. Aliev, Y. Tserkovnyak, T. S. Santos, and J. S. Moodera, Phys. Rev. Lett. **97**, 026602 (2006).
[13] C. Tiusan, F. Greullet, M. Hehn, F. Montaigne, S. Andrieu, and A. Schuhl, J. Phys.: Condens. Matter **19**, 165201 (2007).
[14] The spatial variation of the realistic electronic structure of the Fe–C/MgO interface (related to realistic morphology) will lead to a distribution in energy of the interfacial resonance.
[15] J. A. Stroscio, D. T. Pierce, A. Davies, R. J. Celotta, and M. Weinert, Phys. Rev. Lett. **75**, 2960 (1995).
[16] The interfacial resonance state of Fe has a d_{z^2} orbital character and belongs to the Δ_1 symmetry. However, due to the strong localization of the d_{z^2} band, this state decays rapidly with the MgO thickness. Therefore, for large MgO thickness its contribution to the total AP conductivity is expected to be small.
[17] Ya. M. Blanter and M. Büttiker, Phys. Rep. **336**, 1 (2000).